Int J Clin Exp Med 2015;8(1):598-606
www.ijcem.com /ISSN:1940-5901/IJCEM0003213

*Original Article*

# Orthotopic transplantation of decellularized liver scaffold in mice

Hongyu Zhang*, Yujun Zhang*, Fengxi Ma, Ping Bie, Lianhua Bai

*Hepatobiliary Institute, Southwestern Hospital, Chongqing 400038, China. *Equal contributors.*

Received October 17, 2014; Accepted December 27, 2014; Epub January 15, 2015; Published January 30, 2015

**Abstract:** End-stage liver disease is a life threatening health problem to millions of people worldwide. Orthotopic liver transplantation is the only therapy for the definitive cure at the present time. However, persistent shortage in donor organs limits the opportunity for patients to receive this treatment. Liver tissue engineering aims to overcome this restriction by generating functional tissue constructs for treatment of individuals with the end-stage liver disease. Recently, a new strategy has emerged using the natural organ scaffold as a vehicle for liver tissue engineering. This involves preparation of decellularized scaffold containing the circulatory framework of the natural organ system. Currently, surgical performance of liver scaffold transplantation with end-to-side anastomosis of major vessels in small experimental animals, particularly in mice (mLBST), remains technically challenging. Here, we describe surgical techniques of mLBST that can be used for evaluation of engineered liver grafts in recipients.

**Keywords:** Surgical technique, liver transplantation, liver regeneration, tissue engineering, repair

## Introduction

Using the cuff technique [1] to replace the suturing procedure has been considered as a critical advancement in performing orthotopic liver transplantation (OLT) in rodent models [2-4]. This improvement has significantly shortened the time of blocking the portal vein and increased the survival rate of animals. The success of OLT in mice was achieved in 1991 [5]. Although, techniques of operating microsurgery on mice and on large animals are similar in theory, the procedure of mouse OLT is much more complex and technically dependent. At the present time, technical difficulties of operation remain substantially restricting the application of mouse OLT model in biomedical research. Since mouse OLT model has a number of advantages for biomedical research, including the availability of specific gene engineered mouse strains, the similarity of mouse immune and metabolic characteristics to those of humans, and the convenience of animal care, improvement of surgical technique will enhance the application of mouse OLT model for biomedical research. In light of this understanding, we developed mouse orthotopic liver bioscaffold transplantation (OLBT) model. Here, we report for the first time about key surgical techniques of OLBT in mice. In our studies, we used a combination of hand-suture [2] and cuff [6] techniques to complete end-to-side anastomosis of the portal vein (PV) and the inferior vena cava (IVC). The successful rate of mouse OLBT surgery achieved ~80% in this series.

## Experimental procedures

### *Surgical materials*

All procedures were performed with the aid of an operating microscope with 4× magnification. Other basic instruments required for the procedure include scissors, forceps (fixation forceps, mosquito forceps, Adson's forceps, Kelly's forceps, and Jeweler's forceps), retractors and towel clamps which were purposely prepared according to the goal of each operative step. All instruments were kept on a cork board during surgery to prevent damage to their fine tips. Micro-clips were prepared in several sizes (Shanghai Apparatus & Instrument. Co Limited, China). Threads for surgical suture included thin silk threads (11-0 Ningbo Medical Needle Co Ltd), monofilament nylon suture, monofilament

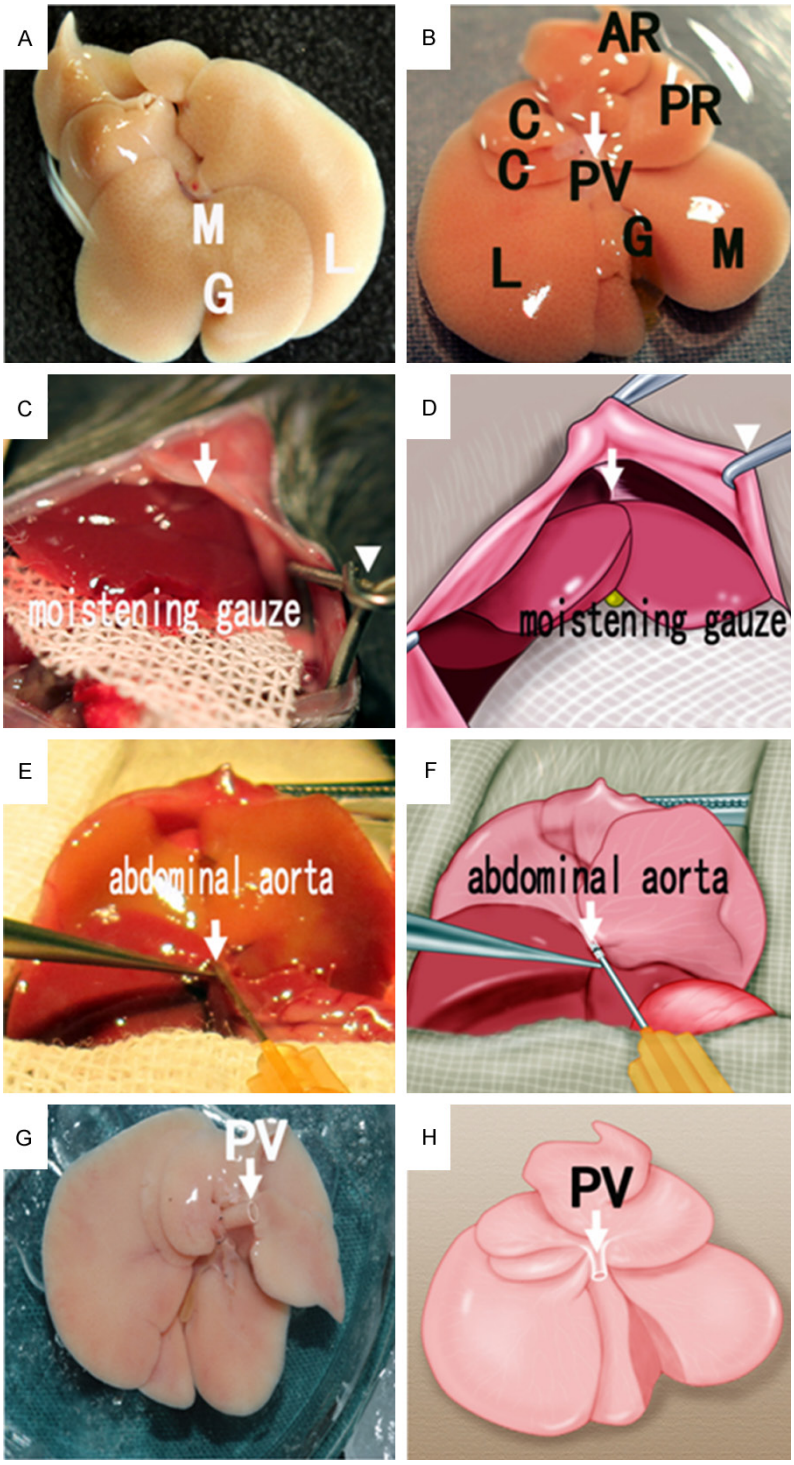


**Figure 1.** Gross anatomy of mouse liver and continuous perfusion of the abdominal aorta with PBS for removing erythrocytes. Detailed front (A) and rear (B) view of excised and illustrated mouse liver. G = gallbladder; M, C, and L = median, caudate and left lobes of the liver, respectively. The right lobe of the liver is divided into two distinct lobes, i.e. anterior right (AR) and posterior right (PR) lobes. PV = Portal Vein. (C) Exposure of liver and placement of moistening gauze. (E) Isolation and cannulation of abdominal aorta. (G) View of liver after removal of erythrocytes by perfusion. (D, F, and H) are illustrations representing (C, E, and G), respectively.

polypropylene sutures and absorbable thread (11-0 Ningbo Medical Needle Co, Ltd). Because sterile conditions were required for the entire surgical procedure, betadine disinfection of the abdominal surgical area was performed. Other chemical agents required for the procedure included heparin lithium salt (100 unit/mg, Southwest Hospital, Chongqing, China), antibiotics (cephalexin hydrate; Pharmacentical North China), analgesic agent (buprenorphine, 100 μg/mL; Sigma, USA), bicarbonate (8.4% sodium bicarbonate injection USP, 1 mEq/ml, 84 mg/ml; Southwest Hospital, Chongqing, China), cotton-like regional hemostatic agent (Shifeng Medical Apparatus & Institute Chengdu Co. Limited, China), Lactated Ringer's solution, Ringer's solution (Otsuka Beijing Research Institute, China) and isotonic normal saline (NS) (0.9% sodium chloride injection USP; Southwester Hospital, Chongqing, China). Peripheral catheters in sizes of 14, 16 and 24 gauge (Shandong Weigo Group Medical Polymer Co, China) were also used.

*Surgical precautions*

Since a large vessel diameter would be convenient for performing anastomosis, male inbred syngeneic C57-BL/6 mice at the age of 10-12 weeks old (25-30 g; Third Military Medical University, Chongqing, China) were used as size-matched donors. Recipient mice were maintained under sodium pentobarbital (intraperitoneal, 60 mg/kg) anesthesia

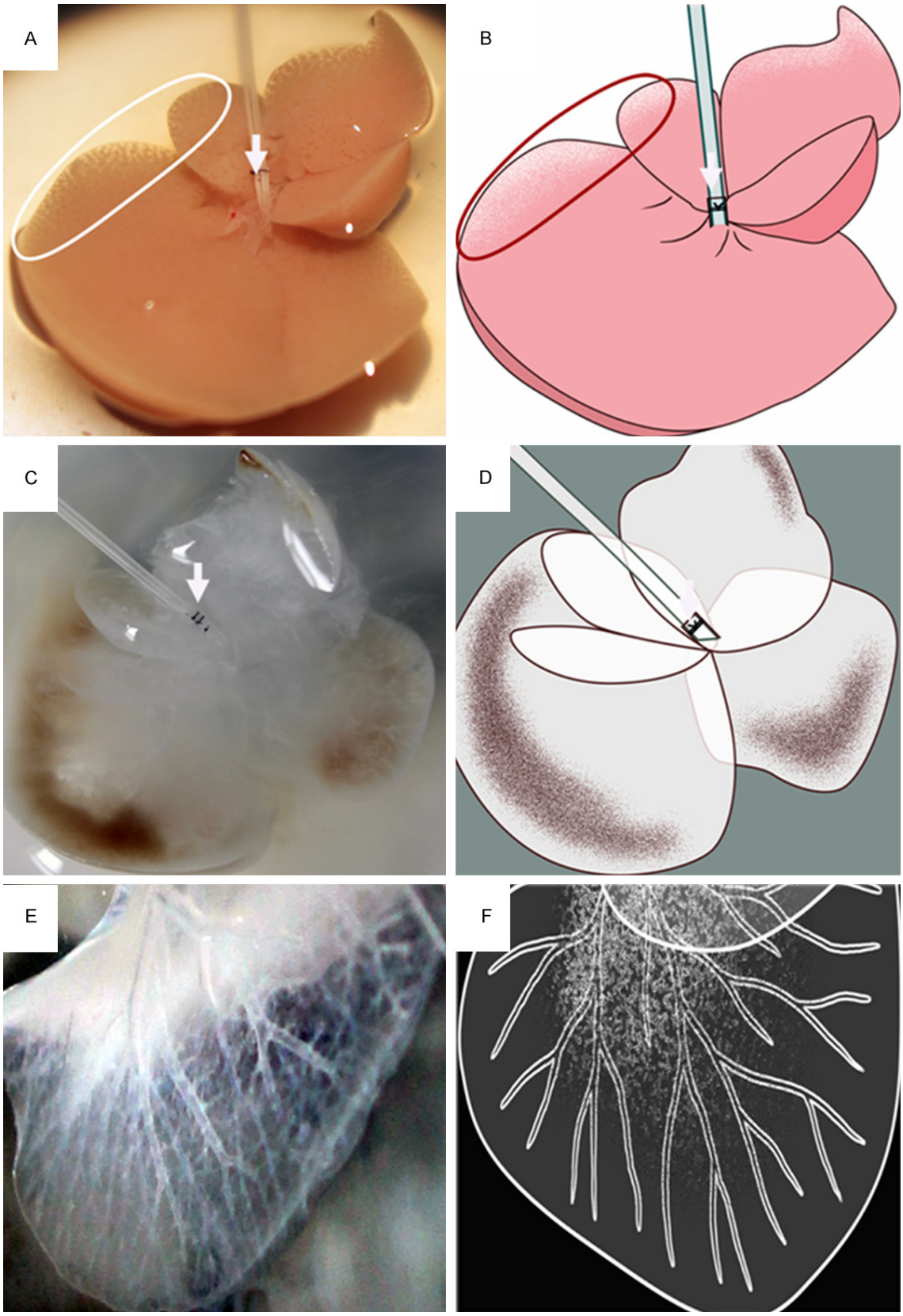


**Figure 2.** Decellularization of mouse liver. Representative images of the decellularization process in excised mouse liver with $dH_2O$ at 2 min (A), with 1% SDS at 48 hr (C), and with $dH_2O$ and PBS at 7.5 hr, totally about 60 hr perfusion (E). (B), (D), and (F) are illustrations representing panels (A), (C), and (E), respectively.

[6-8]. The use of intraperitoneal sodium pentobarbital had the advantage of rapid induction although it was inconvenient in adjusting the depth of anesthesia once being introduced. Mice with a body weight > 33 g were not used as donors because they had a large amount of intra-abdominal fat, making the surgical procedures more difficult. All experimental protocols and procedures were approved by the ethics committee of the Third Military Medical University. Animal handling and care met the requirements of our institutional guidelines for animal welfare (Chongqing, China).

All animals were kept in animal facilities of the Third Military Medical University at least one week prior to surgery to let the mice adjust to the new environment. Mice were then housed in cages at 20 ± 2°C with a 12-hr light-dark cycle and free access to food and water. Deprivation of solid food for 12-24 hrs prior to surgery was conducted in animals in order to avoid extension in the gastrointestinal tract and to reduce the risk of aspiration under anesthesia. The weight of the mice was routinely measured after anesthesia and before surgery using an electronic scale [Sstyptoid Scientific Instruments (Beijing) Co, Beijing, TE601L, Limited China]. A sufficient depth of anesthesia in the absence of asystole, asphyxia, or subsidence of tongue root was essential as the operation included microsurgical procedures. Animals were kept well hydrated prior to surgery as dehydration would easily lead to death during the induction phase of anesthesia. Adequate injections of infusion solutions were important for a successful surgery, particularly prior to the hepatic ligation phase before the PV reflow.

## Results and discussion

### *Preparation of mouse liver decellularized scaffolds*

Sized-matched mice were used as donors. Unlike the rat, the mouse has a gallbladder attached to the liver (**Figure 1A**, **1B**; indicated as G). The hepatic duct from the liver and the cystic duct from the gall bladder unite to form the common bile duct, which extends posteriorly to the duodenum traversing a portion of the pancreas before passing through the duodenal wall to open on a papilla. The mouse liver is divided into four lobes. The largest median lobe (**Figure 1A**, **1B**; indicated as M) is subdivided into right and left portions by a fissure. The falciform ligament locates anteriorly while the gallbladder positions posteriorly in this fissure. The left lobe (**Figure 1A**, **1B**; indicated as L) is between the medial caudate lobe which is partially divided into two leaf-shaped lobes dorsal and ventral to the esophagus at the lesser curvature of the stomach. The right lobe, which is partially divided into anterior (AR) and posterior (PR) lobes, encircles the PV (**Figure 1B**) and the IVC (not shown).

The major aspects of hepatic structure in mice include the hepatic vascular system, the biliary tree, and the three dimensional arrangements of the liver cells. Like human, the circulatory system of the liver in mice is unlike that seen in any other organ. Of great importance is the fact that a majority of blood supply to the liver is venous blood. About 75% of the blood entering the liver is venous blood from the PV. The remaining 25% of the blood supply to the liver is arterial blood from the hepatic artery (HA), a branch of the celiac artery, and the left gastric artery which runs along the esophagus to the liver. Terminal branches of the PV and HA empty together to the sinusoids of the liver. From there the blood flows through the sinusoids and empties into the central vein of each lobe. Central veins coalesce into hepatic veins which leave the liver and empty into the IVC.

After shaving and disinfecting the abdominal area with iodine (Betadine), a long midline skin incision in a donor was made up to an exteriorization of the xiphoid process on the sternum (**Figure 1C**, **1D** indicated as arrows) with the purpose to provide a better exposure for adequate surgical field. Retractors were then utilized to optimize retention of the bilateral costal bows (**Figure 1C**, **1D** indicated as arrowheads). The intestines were covered with moistening gauze (**Figure 1C**, **1D**). The exposed gallbladder and bile duct were then transected. In order to wash out erythrocytes from the liver, the abdominal aorta was identified (**Figure 1E**, **1F** indicated as arrows) and perfused with phosphate-buffered saline (PBS) (5 mL/min) for 30 min. After removing erythrocytes, the liver was carefully removed from the body cavity along with the PV (**Figure 1G**, **1H** indicated as arrows) and IVC in the intact capsule. The PV was cannulated with a 22-gauge infusion tube (Terumo Medical Corp, BD, USA) (**Figure 2A**, **2B**; indicated as arrows) attached to a pump (San Feng

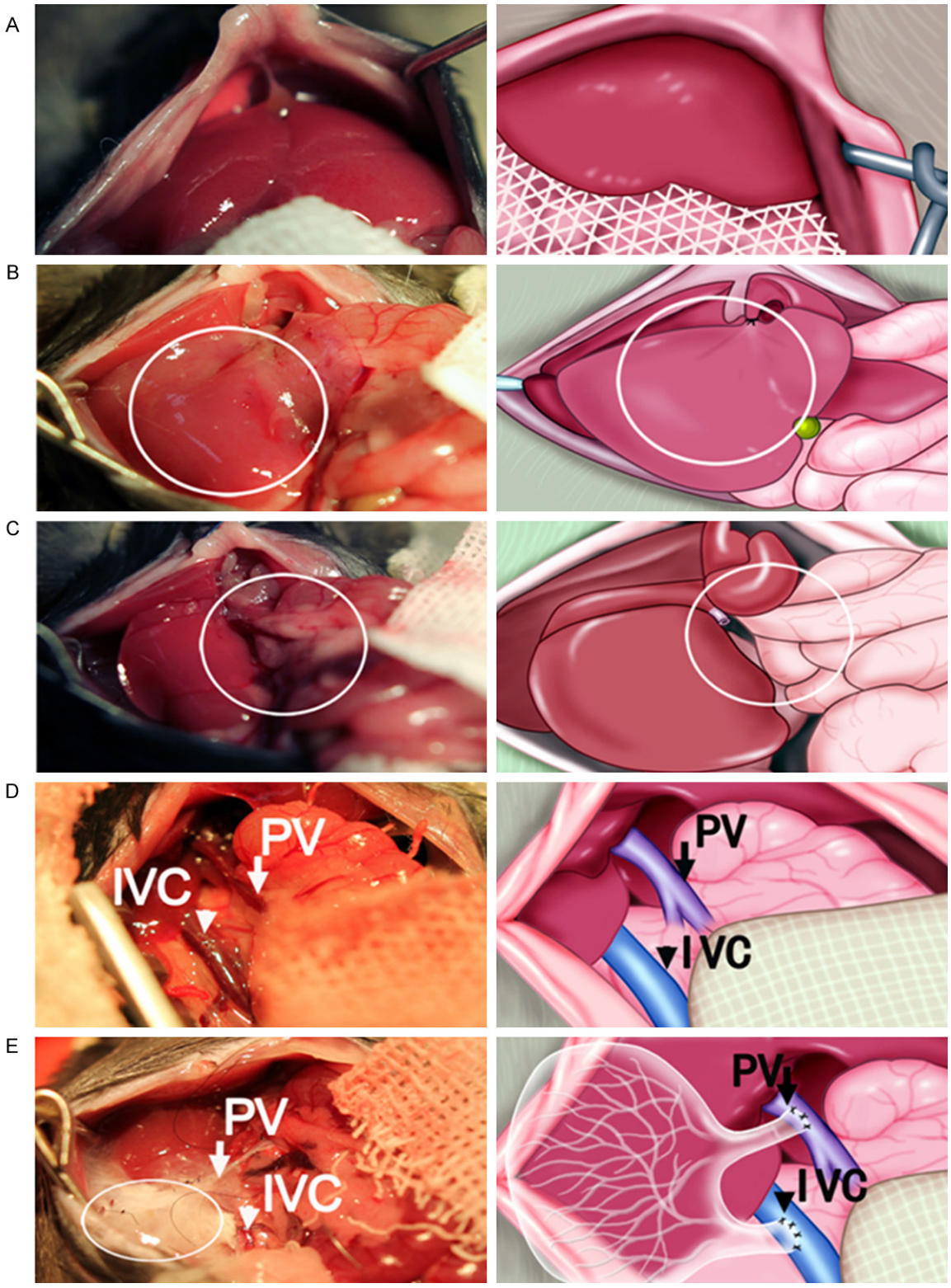


**Figure 3.** Recipient operations for connection of the PV and IVC from the recipient liver to the decellularized liver scaffold through end-to-side anastomosis. A-E. Representative images and illustrations depicting the procedure of end-side anastomosis of the PV and IVC from the recipient liver to the decellularized scaffold. (A) Exposure of recipient liver, (B, C) isolating middle liver lobe (B, indicated as circle) and removing middle liver lobe (30% hepatectomy) (C, indicated as circle), (D) isolation of the PV (indicated as arrows) and IVC (indicated as arrowheads) and (E) reconnection of the PV (indicated as arrows) and IVC (indicated as arrowheads) from the recipient liver to the decellularized scaffold (indicated as circle).

Edward Electric Co. LTD China). The PV was then perfused with distilled water ($dH_2O$) for 2 hr (5 mL/min). Following 2 min of $dH_2O$ perfusion, decellularization was observed at the periphery area of the liver (**Figure 2A**, **2B** area encircled). Subsequently, sodium dodecyl sulfate (SDS) (Sigma-Aldrich)-based perfusion was performed. During a period of 48 hr, SDS solution (1% SDS in $dH_2O$ containing 0.05% Trypson and 0.002% EDTA) in a volume approximately 30 times of the liver was perfused through this circuit (**Figure 2C**, **2D**). The arrow indicates the site of PV cannulation. After perfusion with SDS solution, the liver was perfused with $dH_2O$ for 6 hr to wash out SDS. Finally, the liver was perfused through the PV cannulation with PBS for 1.5 hr to continue decellularizing the lobes until a clear parenchyma with defined liver capsule and vasculature was observed (**Figure 2E**, **2F**). The total amount of perfusion solution used during this process was approximately 45 times of the liver volume. The decellularized liver scaffold was then placed into a container holding 0.3 ml of cold Lactated Ringer's solution containing heparin (100 units) for further preparation.

*Re-connection of the PV and IVC from the recipient liver to the scaffold by end-to-side anastomosis*

A successful surgery to mobilize partial liver can be secured by reducing the hepatic phase (< 20 min, preferable) and the total operative time (< 60 min, preferable) including the time used for HA reconstruction [35]. In our study, the surgical procedure for 30%-60% liver resection (left and middle lobules) took about 2 min and the total operative time was less than 18 min. Initially, a laparotomy was performed to provide a better exposure (**Figure 3A**), in which a skin bilateral subcostal incision with an upper midline T extension was made along the midline. The middle liver lobe was then divided (**Figure 3B**, area encircled) and removed (**Figure 3C**, area encircled). The exact location of the incision was often dictated by the size and configuration of the liver. Once the lobe was removed, exposure of the PV and the IVC was implemented (**Figure 3D**, indicated as arrow and arrowhead, respectively), which was followed by cross-clamping the PV and the IVC, respectively. The maximum length of the vessel was retained within the recipient for the convenience of subsequent vessel reconnection. The decellularized mouse liver scaffold was placed into the site where the lobe was removed. End-to-side anastomosis of the recipient PV with the PV of the scaffold was conducted with a continuous 11-0 nylon suture (Becton Dickinson and Company, BD USA) (**Figure 3E**, indicated as arrows). Connection of the recipient IVC to the IVC of the scaffold by using the same procedure was then performed (**Figure 3E**, indicated as arrowheads). An end-to-side anastomosis technique was used to facilitate visualizing and manipulating the posterior anastomotic wall while avoiding excessive retrograde bleeding during the procedure. Any blood lost during the operation was replaced with Lactated Ringer's solution.

*Re-connection of the HA and bile duct from the recipient liver to the scaffold by end-to-end suture*

The clamp on the PV was removed to allow reflow of the PV system (**Figure 4A**, indicated as arrows). Subsequently, the clamp on the IVC was removed to initiate reflow of the IVC (**Figure 4B**, indicated as arrows). The HA from the scaffold was identified (**Figure 4C**, indicated as arrows). Connection of the recipient HA to the HA from the scaffold was established through an end-to-end anastomosis by hand suturing [9] (**Figure 4D**, indicated as arrows). Biliary continuity was then restored by connecting the ducts with a 4-mm polyethylene tube stent (OD of 0.61 mm, Becton Dickinson; Parsippany, NJ) (**Figure 4D**, indicated as arrowheads). Bile duct drainage was constructed to drain out any leaked bile from the body (**Figure 4E**, indicated as arrow, right panel). The abdomen was finally closed in two layers. Single intramuscular injection of cefamandol nafate (5 mg) and bicillin (60,000 units) was given to each recipient mouse for protection of infection. Recipient mice were kept under a warming lamp until they became active. Food and water were allowed ad libitum.

During the operation period, the gastrointestinal tract was continuously moistened with warm NS. The induction of anesthesia, measurement of body weight, and injection of Lactated Ringer's solution were the same as described for the donor surgical procedure. However, shaving was omitted or performed only over a very small area in recipients in order to maintain body temperature following sur-

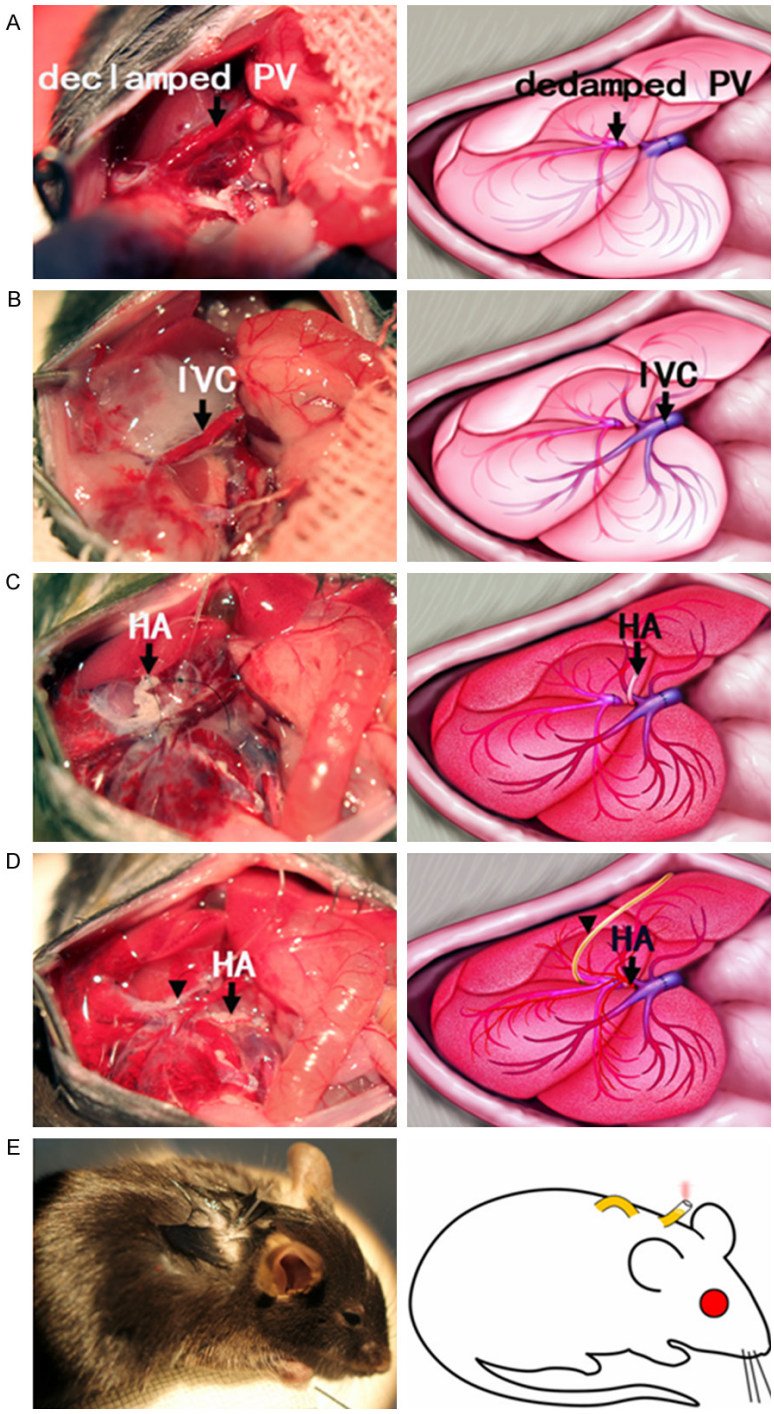


**Figure 4.** Connection of the HA and bile duct from the recipient liver to the scaffold by end-to-end suture. (A-E) Representative images and illustrations depicting the procedure of connecting the HA and bile duct from the recipient liver to the decellularized liver scaffold. Declamping the PV to reflow the blood (A, indicated as arrow), declamping the IVC to reflow the blood (B, indicated as arrow), identification of the HA from the decellularized liver scaffold (C, indicated as arrow), reconstruction of the HA in the decellularized liver scaffold with that in the recipient mouse to allow for reflowing the blood (D, indicated as arrow), and reconnection of the bile duct (D, indicated as arrowhead). Closure of the abdomen and drainage of bile from the body through the bile duct (E, indicated as arrowhead).

gery. Despite NS was indispensable during the procedure, application of NS in a too large volume on the surface of intraperitoneal organs would cause abnormally low body temperature following recipient surgery. As such, only warm NS was used during the surgical procedure. Temporary retention of the abdominal wall by retractors was performed sparingly in order to prevent the restriction of thoracic movements. To our knowledge, this is the first description of a surgical protocol for mLBST. Although surgical techniques are similar between mLBST and rat LRST [10], the current procedure is more difficult due to the smaller size of mouse liver vasculature. We commonly completed end-to-side anastomosis of both PV and IVC within 18 min. The short hepatic period (about 20 min) was important for consistent success, which might reflect the weak tolerance of mice to hepatic ischemia. In contrast, the hepatic period of less than 26 min could be well-tolerated by rats [1]. The lethal surgical complication of the end-to-side anastomosis was hemorrhagic shock during reflow of blood into the liver scaffold via the PV [11]. Our procedure has basically solved this problem.

Our mouse model is expected to be very useful for future studies on transplantation of bioengineered liver. This is strongly supported by the fact that numerous genetically manipulated strains of mice are currently available. In addition, mouse models are widely used for investiga-

tion on the immune responses. Effort in research on liver engineering will also promote the development of regenerative medicine [12], particularly in the field of liver tissue regeneration under pathological conditions [13]. The prospect of evaluating bioengineered liver for therapeutic purposes is equally inviting. Furthermore, our model can be used in conjunction with other unique models of liver diseases in mice, such as viral hepatitis in mice which models human infection with hepatitis viruses [14, 15], to extend the application of our mouse OLBT model to a broad field of biomedical investigation.

## Abbreviations

mLBST, mouse liver bioscaffold transplantation; OLT, orthotopic liver transplantation; OLBT, orthotopic liver bioscaffold transplantation; PV, portal vein; IVC, inferior vena cava; NS, normal saline; HLA, human leukocyte antigen; HA, hepatic artery; PBS, phosphate-buffered saline; SDS, sodium dodecyl sulfate.

## Acknowledgements

This project was supported by the National Natural Science Foundation of China (NSFC). Grant No. 81170425. We thank Xiangdong Lai, Jiejuan Lai at our Institute for the mouse liver scaffold preparation and Linli Zeng for taking care of animals.

## Disclosure of conflict of interest

None.

**Address correspondence to:** Dr. Lianhua Bai, Hepatobiliary Institute, The Third Military Medical University, Southwestern Hospital, No. 30 Gaotan Yan, Shaping Ba District, Chongqing 400038, Sichuan, China. Tel: +86-23-68765808; Fax: +86-2365462170; E-mail: qqg63@outlook.com

## References

[1] Kamada N, Calne RY. Orthotopic liver transplantation in the rat. Technique using cuff for portal vein anastomosis and biliary drainage. Transplantation 1979; 28: 47-50.

[2] Brath E, Miko I, Kovacs J, Toth FF, Fachet J, Furka I. Multiorgan transplantation with a new organ-chip technique in mice: preliminary histological data. Microsurgery 2003; 23: 466-469.

[3] Hori T, Nguyen JH, Zhao X, Ogura Y, Hata T, Yagi S, Chen F, Baine AM, Ohashi N, Eckman CB, Herdt AR, Egawa H, Takada Y, Oike F, Sakamoto S, Kasahara M, Ogawa K, Hata K, Iida T, Yonekawa Y, Sibulesky L, Kuribayashi K, Kato T, Saito K, Wang L, Torii M, Sahara N, Kamo N, Sahara T, Yasutomi M, Uemoto S. Comprehensive and innovative techniques for liver transplantation in rats: a surgical guide. World J Gastroenterol 2010; 16: 3120-3132.

[4] Goto T, Kohno M, Anraku M, Ohtsuka T, Izumi Y, Nomori H. Simplified rat lung transplantation using a new cuff technique. Ann Thorac Surg 2012; 93: 2078-2080.

[5] Uygun BE, Soto-Gutierrez A, Yagi H, Izamis ML, Guzzardi MA, Shulman C, Milwid J, Kobayashi N, Tilles A, Berthiaume F, Hertl M, Nahmias Y, Yarmush ML, Uygun K. Organ reengineering through development of a transplantable recellularized liver graft using decellularized liver matrix. Nat Med 2010; 16: 814-820.

[6] Steger U, Sawitzki B, Gassel AM, Gassel HJ, Wood KJ. Impact of hepatic rearterialization on reperfusion injury and outcome after mouse liver transplantation. Transplantation 2003; 76: 327-332.

[7] Qian SG, Fung JJ, Demetris AV, Ildstad ST, Starzl TE. Orthotopic liver transplantation in the mouse. Transplantation 1991; 52: 562-564.

[8] Humar B, Raptis DA, Weber A, Graf R, Clavien PA, Tian Y. Sewed revascularization for arterialized liver transplantation in mice. J Surg Res 2013; 184: e1-e7.

[9] Ishii E, Shimizu A, Takahashi M, Terasaki M, Kunugi S, Nagasaka S, Terasaki Y, Ohashi R, Masuda Y, Fukuda Y. Surgical technique of orthotopic liver transplantation in rats: the Kamada technique and a new splint technique for hepatic artery reconstruction. J Nippon Med Sch 2013; 80: 4-15.

[10] Zimmermann FA, Butcher GW, Davies HS, Brons G, Kamada N, Türel O. Techniques for orthotopic liver transplantation in the rat and some studies of the immunologic responses to fully allogeneic liver grafts. Transplant Proc 1979; 11: 571-577.

[11] Czabanka M, Ali M, Schmiedek P, Vajkoczy P, Lawton MT. Vertebral artery-posterior inferior cerebellar artery bypass using a radial artery graft for hemorrhagic dissecting vertebral artery aneurysms: surgical technique and report of 2 cases. J Neurosurg 2011; 114: 1074-1079.

[12] Struecker B, Raschzok N, Sauer IM. Liver support strategies: cutting-edge technologies. Nat Rev Gastroenterol Hepatol 2014; 11: 166-176.

[13] Palakkan AA, Hay DC, Anil Kumar PR, Kumary TV, Ross JA. Liver tissue engineering and cell sources: issues and challenges. Liver Int 2013; 33: 666-676.

[14] von Schaewen M, Ding Q, Ploss A. Visualizing hepatitis C virus infection in humanized mice. J Immunol Methods 2014; 410: 50-59.

[15] von Schaewen M, Ploss A. Murine models of hepatitis C: what can we look forward to? Antiviral Res 2014; 104: 15-22.